Vol. 16, No. 3, 2025
ISSN 2233-4203/ e-ISSN 2093-8950
ARTICLE www.msletters.org | Mass Spectrometry Letters

Comprehensive Chromatographic Analysis of Futibatinib Impurities by HPLC and LC-MS/MS: Structural Elucidation, Degradation Kinetics, and *In-Silico* Toxicity Assessment

Sai Kumar Badam[1], Gopala Krishna Murthy Kalapala[2], Srinivasa Kumar Bhavirisetti[3], Sambasiva Rao Tummala[4], and Sreenivasa Rao Battula[1]*

[1]GITAM (Deemed to be University), Department of Chemistry, Visakhapatnam-530045, A.P., India
[2]University of South Dakota, Department of Chemistry, Vermillion, SD-57069, USA
[3]Koneru Lakshmaiah Education Foundation, Department of Mathematics, Guntur-522302, A.P., India
[4]Stira Pharma Private Limited, Regulatory Affairs, Manjeera Trinity Corporate, Hyderabad-500072, Telangana, India

Received August 5, 2025, Revised September 9, 2025, Accepted September 23, 2025
First published on the web September 30, 2025; DOI: 10.5478/MSL.2025.16.3.84

Abstract : A selective and robust High Performance Liquid Chromatography (HPLC) method was developed for the separation and quantification of futibatinib, which is a novel irreversible fibroblast growth factor receptors (FGFRs) inhibitor, and its known impurities. The method optimization involves the evaluation of various chromatographic parameters, and results proved that the Kinetex C18 column and an isocratic mobile phase of acetonitrile and aqueous phosphate buffer (pH 4.1, 65:35 v/v) at 0.8 mL/min were optimal for the resolution of futibatinib and its impurities. The forced degradation studies reveal the susceptibility of futibatinib towards acidic and oxidative conditions. The degradation follows pseudo-first-order kinetics, with maximum degradation recorded under acidic conditions (k = 0.0413 h^{-1}, $t_{1/2}$ = 16.78 h) and then by oxidative stress (k = 0.0331 h^{-1}, $t_{1/2}$ = 20.93 h). Five major Degradation Products (DPs) were identified in which DP 1 (*m/z* 319.7691) is a vinyl halide produced through Markovnikov-type electrophilic addition, DP 2 (*m/z* 391.3912) is a bis-hydroxy derivative produced through oxidative demethylation, DP 3 (*m/z* 365.968) and DP 4 (*m/z* 296.2975) are the products of acid-induced hydrolysis and ring cleavage whereas DP 5 (*m/z* 433.4311) is a nitroso-derivative produced through oxidative modification of the amine group. The in-silico toxicity predictions classify all DPs under toxicity class 4, indicating consistent neurotoxic and carcinogenic potential, whereas DP 4 and 5 show mutagenic and immunotoxin risks. This study offers the first comprehensive degradation profiling of futibatinib by providing a stable analytical platform for quality control, regulatory compliance, and formulation stability.

Keywords : Futibatinib, Impurity profiling, Mass characterization, Toxicity assessment

Introduction

The pharmaceutical impurities that may arise in the manufacturing process, aging over a period of time, or storage conditions, are a major issue that influences the drug quality as well as patient safety. The regulatory bodies like the International Council for Harmonisation (ICH) emphasize the need to detect, quantify, and evaluate the safety levels of these impurities. According to ICH, any of these impurities that exist at a higher than prescribed level must be identified and assessed.[1] These impurities can change the functioning of a drug and may even cause harmful effects or reduce its effectiveness. Therefore, study and control of these impurities is treated as a crucial part of drug development and quality assurance. In this regard, advanced chromatographic methods such as HPLC/ Ultra Performance Liquid Chromatography (UPLC) and Liquid Chromatography-Tandem Mass Spectrometry (LC-MS/MS) play a key role in the discovery of safe drugs. HPLC is widely used for the separation and quantification of trace-level impurities and DPs with high accuracy, whereas LC-MS/MS helps to identify unknown DPs by providing detailed molecular and structural information. The combination of these techniques offers a powerful approach to understanding impurity profiles and degradation pathways that supports the development of reliable, stability-indicating methods for routine testing and regulatory approval.[2]

The rise in demand for target cancer therapy has driven

*Reprint requests to Sreenivasa Rao Battula
https://orcid.org/0000-0002-0242-5032
E-mail: sbattula2@gitam.edu

the development of tyrosine kinase inhibitors (TKI), which are a class of drugs that have revolutionized oncology, offering more selective and effective treatment strategies. One such TKI, Futibatinib, has garnered considerable attention due to its potent and irreversible inhibition of FGFRs, especially FGFR2.[3] It was prescribed to treat intrahepatic cholangiocarcinoma (bile duct cancer within the liver) and other malignancies. It is chemically described as *(E)-N-(3-(6-(4,6-dimethoxy-2-(methylamino)pyrimidin-5-yl)thieno[3,2-d]pyrimidin-4-yl)phenyl) acrylamide*. It demonstrates clinical efficacy and manageable safety in patients with FGFR-driven cancers, and it represents a significant advancement in precision oncology targeting FGFR abnormalities.[4] It is generally well-tolerated medicine but can cause several side effects such as hyperphosphatemia, or elevated phosphate levels in the blood. The patients may also experience gastrointestinal disturbances such as nausea, vomiting, diarrhoea, and constipation. The other frequent side effects, such as fatigue, loss of appetite, dry mouth, stomatitis (mouth inflammation), and dysgeusia (altered taste sensation), were also reported during the usage of futibatinib.[5-6] Futibatinib is a small-molecule drug with a quinoline ring system and an electrophilic acrylamide group. Its structure contains functional groups prone to hydrolytic and oxidative degradation that necessitate the stress stability studies under conditions prescribed by ICH Q1A(R2) guidelines.[7] The DPs formed under these conditions can exhibit toxicological liabilities that need to be characterized and evaluated. Owing to its clinical relevance, the development of a robust analytical framework for the identification and characterization of futibatinib, its impurities, and DPs is imperative to ensure safety, efficacy, and regulatory compliance.

Recent literature has highlighted the increased application of *in-silico* toxicological assessment tools for the early prediction of potential adverse effects of pharmaceutical impurities. Computational methods such as Toxtree, Derek Nexus, and ADMET Predictor allow rapid screening of

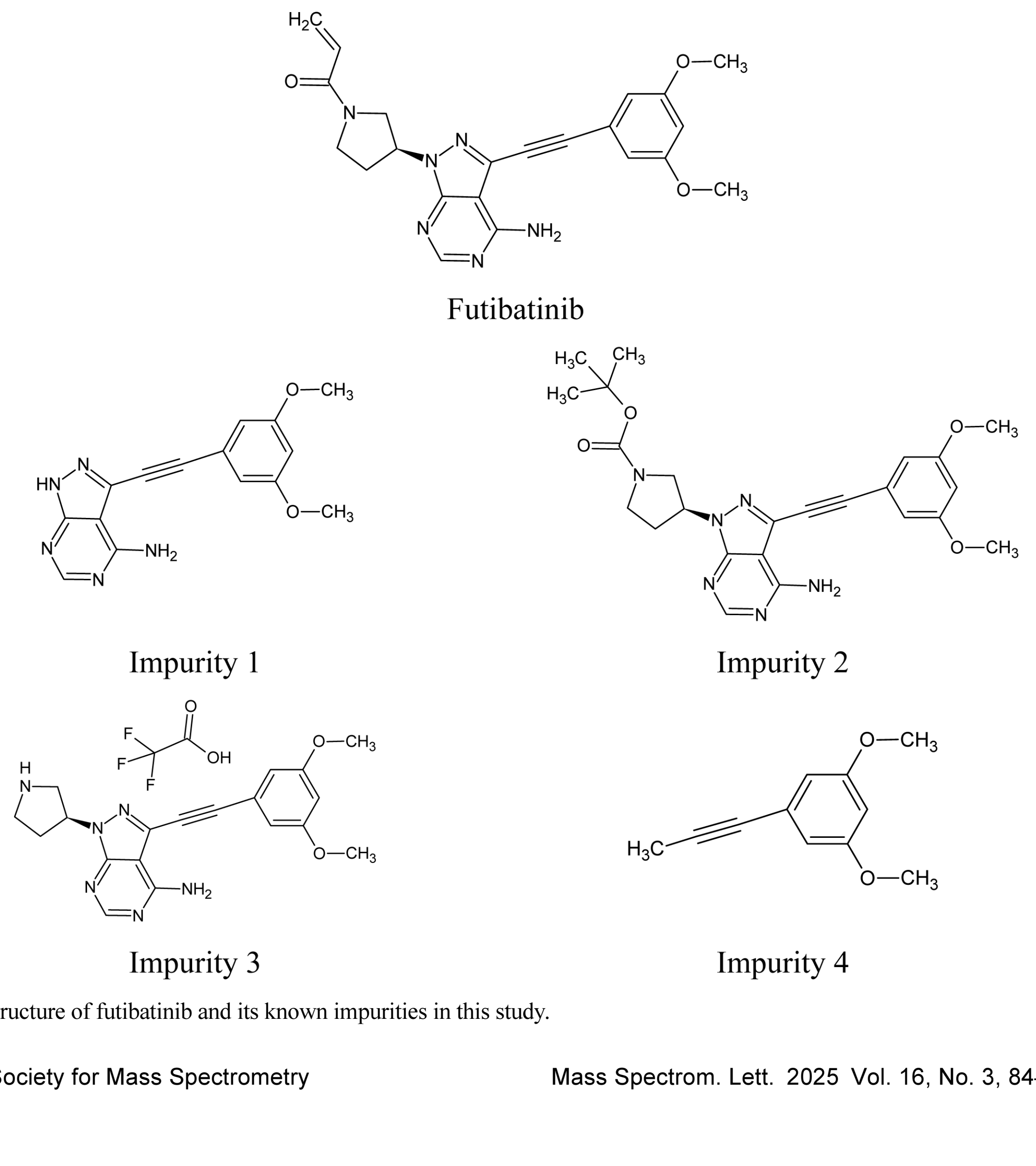

Figure 1. Structure of futibatinib and its known impurities in this study.

mutagenic, carcinogenic, and other toxicological endpoints based on molecular structure and chemical reactivity. The incorporation of *in-silico* study into impurity profiling provides an efficient and cost-effective alternative to labour-intensive *in-vivo* toxicological studies.

Despite its therapeutic promise, there is a scarcity of detailed analytical studies on futibatinib with a special focus on impurity profiling and degradation behaviour of futibatinib. In literature, limited work has been reported on quantification of futibatinib in various biological samples using HPLC-MS[8], UPLC-MS/MS[9], UPLC-MS/MS[10], and LC-ESI-MS/MS method in combination with binimetinib.[11]

No reported method offers a study related to forced degradation of futibatinib, structural characterization, and toxicity prediction of its DPs. This gap necessitates a methodical approach combining advanced chromatographic and spectrometric techniques with *in-silico* modelling to develop a complete impurity profile of futibatinib. Hence, the present study aimed to fill this gap by developing and validating a stability-indicating HPLC method for the separation and quantification of futibatinib and its impurities. Additionally, the LC-MS/MS technique was employed for the structural elucidation of major DPs generated under stress conditions. The degradation kinetics were evaluated to understand the rate and extent of degradation under various environmental conditions. Furthermore, the toxicity profiles of identified DPs were assessed using *in-silico* tools that align with contemporary trends in predictive toxicology. Figure 1 provides the structure of futibatinib and its impurities selected in this study.

Materials and Methods

Solvents, standards, and reagents

The pure samples of futibatinib (with a confirmed purity of 98.25%) and its known impurities, namely impurity 1 to 4, along with marketed futibatinib tablets (Lytgobi® - 4 mg strength), from Actiza Pharmaceutical, Surat, Gujarat, India. The solvents used for HPLC analysis, such as acetonitrile, methanol, and water of HPLC grade, substances were as well as the necessary buffer substances, were purchased from Merck Life Science Private Limited, Mumbai, India. Additionally, chemicals required to conduct forced degradation experiments, such as sodium hydroxide (NaOH), hydrogen peroxide (H_2O_2), and hydrochloric acid (HCl), are of analytical grade and were also acquired from the same supplier.

Apparatus

The HPLC system equipped with UV was utilized for the analysis of futibatinib. A Shimadzu system that includes a quaternary pump, auto-injector, vacuum degasser, and SPD 10Avp UV-Visible detector was utilized in this study. This setup was connected to a computer operating with N2000 software for instrument control, data acquisition, and analysis. The chromatographic separation was achieved using a Kinetex C18 column analytical column with dimensions of 250 × 4.6 mm and a particle size of 5 µm at room temperature. The 0.80 mL/min isocratic flow of acetonitrile and aqueous phosphate buffer in 65:35 (v/v) as mobile phase. The column eluents were recorded through UV detector at 229 nm and the analysis was completed within a total run time of 12 min.

The MS/MS analysis was performed on Waters SYNAPT G2-Si high-definition quadrupole time-of-flight (Q-TOF) mass spectrometer (Waters, USA) equipped with an electrospray ionization (ESI) source at positive ion mode. The mass spectrometer was calibrated using sodium formate solution and real-time mass correction was performed using Leucine Enkephalin (*m/z* 556.2771 in positive mode. Data acquisition was carried the MS-E mode that alter between low-energy (collision cell off) and elevated-energy (20–40 eV ramp) conditions to generate both precursor and fragment ion information in a single injection. The capillary voltage of 3.0 kV, cone voltage of 35 V, source temperature of 120°C, desolvation temperature of 350°C, desolvation gas (nitrogen) flow of 800 L/h, and cone gas flow of 50 L/h were utilized as optimized ESI source parameters during the analysis. The data acquisition and processing were performed through Waters MassLynx 4.1 software with integrated UNIFI software platform for accurate mass measurement, elemental composition analysis, and structural elucidation.

The compatibility of chromatographic system with the mass spectrometer was ensured by utilizing a post-column split. This split ensures that the Q-TOF instrument receives approximately one-fifth of the total eluent flow (≈1:5 split ratio) and thereby prevent overloading of the ion source. The injection volume was reduces to 5 µL to maintain optimal peak shape and to minimize ion suppression effects in the ESI source. The retention times (RTs) and relative retention times (RRTs) of analyte peaks obtained in the LC-UV chromatogram were directly compared with those observed in the MS chromatograms to identify and confirm the compounds.

Preparation of solutions

The separate stock solutions for futibatinib and its identified impurities were prepared by accurately dissolving each reference material in methanol to achieve a final concentration of 1000 µg/mL. These solutions were stored at a temperature of 0°C in a freezer to preserve their chemical stability throughout the analytical process. An appropriate dilution of these stock solutions was carried out using deionized water to achieve final concentrations of futibatinib in the working solutions ranging from10 µg/mL to 70 µg/mL, whereas impurities in the concentration range of 0.1 µg/mL to 0.7 µg/mL. The calibration standards were prepared by mixing equal volumes of the respective linearity level solutions for each compound. 20 µL volume from each calibration mixture was injected into the HPLC system, which was under the optimized chromatographic settings. Each concentration level was analyzed in triplicate to ensure consistency and reliability of the results.

Preparation of assay sample

Five Lytgobi® tablets, each tablet containing 4 mg of futibatinib, were weighed precisely to determine the average weight of a single unit. An amount of the powdered tablet equivalent to 50 mg of futibatinib was accurately transferred into a 50 mL volumetric flask. To this, approximately 30 mL of methanol was added to the flask to dissolve the active ingredient. This mixture was then subjected to sonication for 5 min to enhance the drug solubility in the solvent. After sonication, the volume was adjusted to 50 mL using methanol to obtain a homogeneous solution. Then, the resultant mixture was filtered through a 0.22 µm membrane filter to remove any insoluble excipients or particulate matter that could interfere with the analysis. An appropriate portion of the filtrate was further diluted to prepare a test sample with a final concentration of 100 µg/mL of futibatinib. This sample solution was analyzed under the same chromatographic conditions as described earlier to ensure the method's reliability to quantify futibatinib and its impurities in formulation samples.

Stress degradation study

The stability of futibatinib under various stress conditions was evaluated according to the ICH guidelines Q1A(R2), through forced degradation studies.[12-14] This test was conducted to assess the drug's behavior when exposed to harsh environments as well as to identify potential DPs formed in these conditions. These studies are also essential to determine the method's effectiveness to differentiate futibatinib from its DPs and thereby confirm its stability-indicating properties. In each stress condition, 1 mL of a concentrated futibatinib (1,000 µg/mL) stock solution was used. This solution was then subjected to the respective stress conditions, and after degradation, the samples were neutralized wherever necessary and then diluted with deionized water to a final concentration of 100 µg/mL in 10 mL volumetric flasks before chromatographic analysis.

In acidic stress testing, 1 mL of 2 M HCl was added to the drug solution, and the mixture was heated at 60°C in a water bath for 30 min. Then it was kept at room temperature for an additional 12 hours to allow further degradation. In the case of alkaline stress, the procedure described in acid stress was followed by replacing HCl with 0.1 M NaOH. The oxidative stability was examined by mixing 1 mL of 30% H_2O_2 with 1 mL of the futibatinib solution, and the resultant mixture was incubated at 60°C for 2 hours in a water bath, followed by cooling to room temperature. The 1 mL of standard stock solution of futibatinib was mixed with 1 mL of deionized water to evaluate its stability under neutral hydrolytic conditions. This mixture was then heated at 80°C in a water bath for 30 min and later allowed to reach ambient temperature. The photolytic degradation was studied by placing 1 mL of the stock solution in a closed 10 mL volumetric flask and exposing it to direct sunlight for 4 hours, whereas thermal degradation was assessed by heating the pure futibatinib powder in a hot air oven at 100°C for 2 hours.

Investigation of degradation kinetics

A degradation kinetics study was carried out to assess the degradation of futibatinib over time when it was exposed to acidic and peroxide conditions.[14-16] In this experiment, individual 1 mL portions of a prepared stock solution of futibatinib within the validated linear concentration range were subjected to acidic and peroxide stress separately. The stressed samples were left to stand at room temperature, and specific volumes were withdrawn at different time intervals to monitor how quickly the drug broke down under these conditions. At each chosen time point, the reaction was immediately neutralized to stop the further degradation of the drug. The neutralized samples were then diluted with deionized water up to 10 mL in volumetric flasks to bring the concentration within the acceptable range for analysis. This sample analysis was processed under the previously optimized chromatographic conditions. The amount of futibatinib remained in each time-based sample was quantified by correlating with the regression equation obtained from the standard calibration curve. A graph was plotted using drug concentration on the Y-axis and time on the X-axis to visualize the rate and pattern of degradation. The obtained plot provides the reaction order and the degradation rate constant in both the peroxide and acid stress studies. The insights gained from this study help to understand the stability characteristics of futibatinib and enable the prediction of its shelf life under acidic storage or handling conditions.

***In-silico* toxicity prediction**

A computer-based toxicity prediction method was employed to evaluate the potential harmful effects of DPs of futibatinib characterized in this study. This analysis was carried out using an online platform called ProTox-II, which is a widely recognized web-based tool to predict the toxicological behavior of chemical substances based on their molecular structures. The ProTox-II tool provides the LD_{50} values of DPs, which refers to the lethal dose required to cause death in 50% of a test group of animals, and was expressed in mg of substance per Kg body weight (mg/kg). This value provides a quantitative understanding of the acute toxicity of each DP. In addition to the LD_{50} values, the software also assigns a toxicity class that ranges from Class 1 (indicates extremely toxic) to Class 6 (indicates relatively non-toxic). These classifications help to categorize the health risk associated with potential exposure to the DPs. The results of this computational analysis offer valuable insights into the safety profile of futibatinib.[17,18]

Statistical Analysis

All required statistical evaluations and data analysis were performed using the built-in functions and features provided in Microsoft Excel 365. This software was utilized to calculate mean values, standard deviations, regression equations, and to generate calibration curves and graphical representations of the results. Additionally, the potential toxicity of the identified DPs was assessed through the Pro-Tox-II online platform.

Results and Discussion

Method optimization

In the current research work, a selective analysis of diverse chromatographic variables was experimented with for designing a durable HPLC technique that possesses the ability to separate futibatinib with its known DPs and impurities. Columns like Waters Symmetry C18 and Kinetex C18 column with length 250 mm and 150 mm × 4.6 mm were evaluated during the column testing stage. Different combinations of methanol, acetonitrile, and phosphate buffer were tested to determine their impact on the separation quality of futibatinib and its impurities. The preliminary trials show that both columns produce similar retention characteristics for futibatinib and its impurities. However, the Kinetex C18 column exhibits enhanced performance in terms of peak sharpness, symmetry, and signal strength. Hence, the Kinetex C18 column was chosen for subsequent method optimization.

The effect of pH in the aqueous component of the mobile phase was investigated to enhance the separation efficiency of the method. The aqueous phase pH range of 3 to 9 was tested to assess its influence on the retention time, peak area, and overall resolution of futibatinib and its impurities. The peaks for futibatinib and its impurities were closely eluted, with poor symmetry observed under a high acidic pH of 3. This is likely due to the complete protonation of analytes at low pH, which diminishes their interactions with the stationary phase, leading to faster elution with distorted peak shapes. The peak broadening with very low resolution was noticed due to partial ionization and instability of the analytes at the basic pH of 8 and 9. Among all the tested conditions, a slightly acidic to near-neutral pH range of 4 and 5 provides the best separation with improved peak resolution, better shape, and consistent retention.

During the next stage of method development, several organic solvents were tested to evaluate their effect on the quality of the peaks and the overall chromatographic performance. The methanol and acetonitrile were tested separately as possible organic modifiers in the mobile phase, and among these solvents, acetonitrile provides better results by considerably improveing the resolution between futibatinib and its impurities. The peaks obtained with acetonitrile show improved shape and intensity, which makes it the preferred organic component for this method. The elution technique was also optimized during this process, and an isocratic elution approach was proved to be adequate for analyzing futibatinib and its impurities. Based on the collective optimization studies, the final chromatographic conditions consist of a Kinetex C18 column (250 mm × 4.6 mm, 5 µm) with 0.80 mL/min isocratic flow of acetonitrile and aqueous phosphate buffer at pH 4.1 in a 65:35 volume ratio, and detection was performed at 229 nm, which corresponds to the absorption maximum (λ_{max}) of futibatinib and its impurities. The total analysis time was 12 min that ensures the efficient separation within a short run.

The system suitability tests were performed using a freshly prepared standard solution of futibatinib and its impurities to ensure the reliability and robustness of the developed method. The chromatographic system (Figure 2)

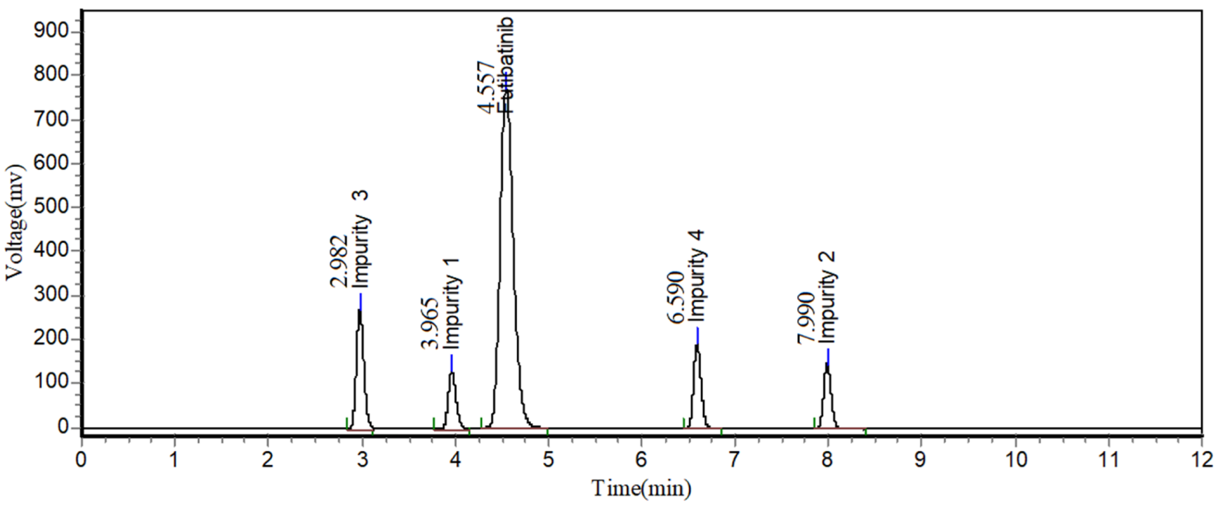

Figure 2. System suitability test chromatogram of futibatinib and impurities.

Table 1. System suitability test results observed for futibatinib and impurities.

Parameter	Futibatinib	Impurity 1	Impurity 2	Impurity 3	Impurity 4
t_R in min	4.5	3.9	7.9	2.9	6.5
Tailing factor	1.03	1.02	0.96	0.95	0.99
Theoretical plates	9936	7201	19752	5891	16308
Resolution	3.47	7.81	9.82	--	15.32

Average results of three experiment (n = 3)

produces sharp, well-resolved peaks for all the components within an acceptable retention time. These system suitability criteria, such as retention time reproducibility, peak symmetry, tailing factor, resolution, and column efficiency, were in line with the specified requirements (Table 1), suggesting the acceptability of the method.

Stress degradation study

A comprehensive forced degradation study of futibatinib was conducted to assess its chemical stability and determine possible DPs generated under different stress conditions. The method developed in this study was utilized as a tool for tracking the degradation behavior of futibatinib under each stress test. In acidic conditions, futibatinib exhibits significant degradation, with a recovery of 63.42%, corresponding to 36.58% degradation. The chromatogram shows the appearance of four distinct and well-separated degradation peaks, confirming the susceptibility of futibatinib under acidic hydrolysis (Figure 3A). In the alkaline environment, the drug displays 94.57% recovery, with 5.43% degradation, and the chromatographic analysis reveals that no DPs were formed in this stress study. When exposed to dry heat, futibatinib retains 97.64%, the photolytic condition displays 95.09% assay, and the neutral conditions retain 68.67% suggesting the stability of the molecule in these conditions. No new degradation peaks were observed under these three stress conditions, suggesting that futibatinib remains chemically stable in such environments. The oxidative degradation retains 70.43% with a % degradation of 29.57%. This procedure yields two DPs (Figure 3B). These results suggest that the drug is more prone to degradation in acidic and peroxide environments, and the summary of degradation behavior under different stress conditions is presented in Supplementary file T1.

Degradation kinetics

A detailed investigation was conducted to assess the breakdown of futibatinib under acid and peroxide (oxidizing) stress conditions. These studies are crucial for evaluating the chemical stability of futibatinib and the stress was simulated with controlled amounts of acid and peroxide. The samples were withdrawn at fixed time intervals from the reaction mixtures and then analyzed using the proposed method. This approach allows the precise monitoring of drug degradation at a point in time (Ct) in comparison to the initial quantity (Co). The analysis reveals a consistent and noticeable decline in the concentration of futibatinib over time in both acidic and oxidative conditions, which indicates the chemical instability of the drug under these stress factors. The data were plotted by taking the logarith-

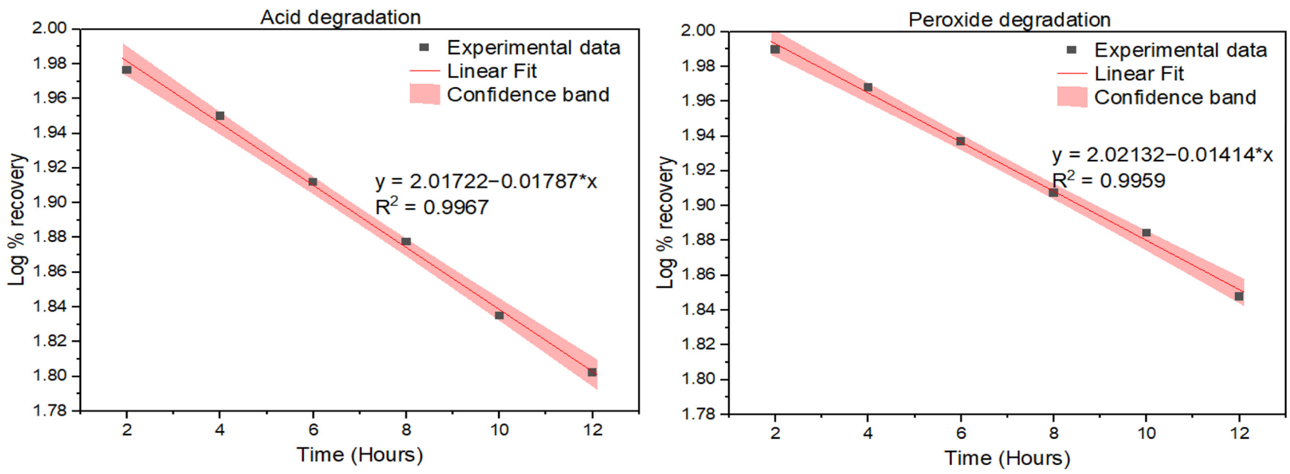

Figure 3. Kinetic plots of futibatinib degradation under stress conditions, showing the degradation profile in acid hydrolysis (A) and peroxide oxidation (B) observed in the optimized method.

mic values of the remaining drug concentration against time, and as a result, straight-line graphs were observed in both conditions. This linearity ensures that degradation follows pseudo-first-order kinetics, which is a simple model applied in describing degradation reactions. The rate at which the drug degraded was termed the rate constant (k) and derived from the gradient of these plots. The k was determined to be 0.0413 h^{-1} with half-life ($t_{1/2}$) of 16.78 hours in acid-induced degradation, whereas the oxidative degradation shows a rate constant of 0.0331 h^{-1} with half-life of 20.93 hours. This result clearly suggests that futibatinib degrades more rapidly in acidic conditions than in oxidative condition. This test finding emphasizes the need to preserve the drug from acid and oxidative conditions during formulation and storage to maintain its stability. The graphical illustration of the degradation kinetics under acid and oxidative stress conditions is presented in Figures 3 respectively.

Method Validation

The sensitivity of the method was carefully examined to evaluate the efficiency of the analytical method to detect and quantify very small amounts of impurities in the study. This was verified by identifying LOD and LOQ of impurities by utilizing the signal-to-noise ratio approach. The method exhibits excellent capability to identify and accurately quantify impurities at extremely low levels, demonstrating its sensitivity. Specifically, the LOD for the impurities was determined to be 0.03 μg/mL, and the LOQ was 0.10 μg/mL. This result indicates that the method is highly effective to detecting even minute quantities of impurities.

In addition to sensitivity, the method's reliability to measure different concentrations of futibatinib and its impurities was also validated in a linearity study. The result shows a strong and consistent linear relationship across 10 μg/mL to 70 μg/mL for futibatinib and 0.1 μg/mL to 0.70 μg/mL for impurities. The regression equation for futibatinib was achieved to be $y = 17391x + 7983.1$, with a correlation coefficient (R^2) of 0.9995 whereas the regression equation of impurities was noticed to be $y = 50207x + 3.9167$ ($R^2 = 0.9993$) for impurity 1, $y = 70680x + 47.717$ ($R^2 = 0.9997$) for impurity 2, $y = 82131x + 1120.6$ ($R^2 = 0.999$) for impurity 3 and $y = 115957x + 1608.4$ ($R^2 = 0.9991$) for impurity 4. In addition, the % RSD of the slope of the calibration curve was found to be below the acceptable limit of 2%. The low % RSD demonstrates that the slope of the calibration curve was stable and consistent with very nominal variations. These results proved that the method was not only sensitive but also accurate for the determination of futibatinib and its impurities.

The precision and accuracy of the method were tested by intra-day and inter-day studies at three concentration levels. Intra-day testing was done by triplicate analysis on the same day, whereas inter-day testing was conducted within three consecutive days. The method accuracy was determined by relative error (Er) and precision by %RSD. The Er and % RSD of futibatinib and its impurities were reported to be than 2%, which validated the reliability of the method. The recovery results were varied within 98% to 102% which proves good accuracy and reproducibility of the method. Robustness was proved by making small intentional changes to chromatographic conditions like detection wavelength, pH, ratio of solvents, and flow rate. These changes did not impact the results significantly and produced uniform peak areas (%RSD < 2%) and constant retention times with permissible system suitability. This result ensures the robustness of the method under changing conditions.

The method specificity was evaluated by interference testing with common excipients, and the results suggest the absence of interfering peaks at the retention time of the analytes. A standard addition test also proved correct impurity recovery without matrix interference, providing the high selectivity and applicability of the method to routine quality control in complex formulations.

LCMS/MS analysis of DPs

The analytical HPLC method conditions proposed in this study were utilized for LC-MS/MS characterization of DPs. In acidic conditions, futibatinib undergoes degradation through an electrophilic addition reaction with hydrochloric acid. Futibatinib, exposed to one equivalent of HCl, the triple bond in the molecule reacts according to Markovnikov's rule, in which a proton (H^+) is added to the carbon with more hydrogen atoms to form a more stable carbocation intermediate. The chloride ion (Cl^-) then attacks this carbocation, resulting in the addition of chlorine across the triple bond. This leads to the formation of a vinyl halide (R–CH=CH–Cl) as the major degradation product, which was designated as **DP 1** and was identified at 0.9 min in the acid degradation chromatogram. The MS/MS spectrum of DP 1 exhibits experimental mass at *m/z* of 319.7691 (m+1) that establishes its molecular mass as 318 g/mol, corresponds to the molecular formula of $C_{14}H_{15}ClN_6O$. The molecular formula containing chlorine is indicative of the electrophilic addition of HCl across a triple bond, leading to the formation of a vinyl chloride-type structure. The major fragment ions observed at *m/z* 293.7435, 239.6961, 226.2288, 202.2074, 161.6240, and 112.1246 further confirm the breakdown pattern of the parent molecule and support the proposed structure. This data strongly supports that the compound is a vinyl halide derivative of futibatinib that was formed by Markovnikov-type addition of HCl to the alkyne moiety. The compound was confirmed as 1-{(3S)-3-[4-amino-3-(2-chloroethenyl)-1H-pyrazolo[3,4-d]pyrimidin-1-yl]pyrrolidin-1-yl} prop -2-en-1-one, its MS/MS data presented in Table 3. Observed mass spectra are given in supplementary files S2 to S6 for DP 1 to DP 5.

The **DP 2** was identified at an RRT of 0.482 in the chromatogram of both acid and peroxide stress studies due to the cleavage of the methoxy groups ($-OCH_3$) present on the aromatic rings of futibatinib. In these conditions, both methoxy groups undergo demethylation and convert into hydroxyl groups ($-OH$), which leads to the formation of dihydroxy derivatives of the parent compound. This transformation results in a more polar degradation product that was eluted at an elution time of 2.1 min. The HRMS data reveal an $[M+H]^+$ ion at *m/z* 391.3912, corresponding to the molecular formula $C_{20}H_{20}N_6O_3$, with an error of 0.255 ppm. The MS/MS fragmentation pattern supports the proposed structure, with key fragment ions at *m/z* 283.2768 ($C_{14}H_{12}N_5O_2$), indicating the cleavage of part of the side chain. The fragments noticed at *m/z* 231.2420 ($C_{12}H_{12}N_3O_2$) and *m/z* 163.1647 ($C_9H_8O_2$), respectively, due to the loss of aryl and heterocyclic moieties in the structure. The smaller fragments such as *m/z* 151.1606 ($C_6H_8N_5$), 112.1180 ($C_6H_7O_2$), and 111.1365 ($C_5H_8N_3$) arise due to the breakdown of the modified aromatic and nitrogen-containing ring systems. These fragmentation patterns, along with the molecular formula, confirm the structure of DP 2 as a bishydroxy derivative of futibatinib. Table 3 provides its proposed structure along with its MS/MS data.

Futibatinib undergoes a degradation reaction by cleaving the N–C bond within the *1-(pyrrolidin-1-yl)prop-2-en-1-one* moiety in the presence of HCl. This hydrolytic process leads to the detachment of the *prop-2-enal* fragment from futibatinib, which results in the formation of **DP 3**. Subsequently, further degradation of DP 3 occurs through the cleavage of the pyrrolidine ring that eliminates the nitrogen-containing group from the molecule and leads to the formation of **DP 4**. These DP 3 and DP 4 were identified at an RRT of 0.718 and 0.788, respectively. The HRMS analysis confirms the proposed mechanism and possible structure of DP 3 and 4 identified in the study. The DP 3 shows $[M+H]^+$ ion at *m/z* 365.968 with molecular formula of $C_{19}H_{20}N_6O_2$, whereas DP 4 shows $[M+H]^+$ ion at *m/z* 296.2975 with formula of $C_{15}H_{13}N_5O_2$. The parent ion peaks confirm the structural change observed in acid stress and possible loss of the side chain in futibatinib due to acid stress.

The MS/MS fragmentation analysis of DP 3 reveals a clear pattern of breakdown that supports the proposed molecular formula $C_{19}H_{20}N_6O_2$. A major fragment ion at *m/z* 310.3226 ($C_{16}H_{15}N_5O_2$) suggests the loss of the pyrrolidinyl group, which indicates the retention of the heterocyclic and oxygenated core structure. The significant fragment at *m/z* 229.2531 ($C_{11}H_{12}N_6$) was noticed due to the breakdown of methoxy-substitutions from the main molecule. In the spectrum, a prominent peak at *m/z* 174.1746 ($C_8H_7N_5$), 134.1505 ($C_7H_7N_3$), and 124.1353 ($C_5H_7N_4$) was observed.

The MS/MS spectrum of DP 4 displays a parent fragment at *m/z* 296.2975, corresponding to the proposed molecular formula of $C_{15}H_{13}N_5O_2$. A key fragment ion observed at *m/z* 242.2453 ($C_{13}H_{11}N_3O_2$) indicates the loss of a nitrogen-containing fragment, suggesting the cleavage at the pyrrolidine moiety. The appearance of a prominent peak at *m/z* 162.1767 ($C_{10}H_9O_2$), observed twice, indicates the presence of a stable aromatic fragment containing two oxygen atoms that represents a substituted phenolic structure. Another significant fragment at *m/z* 105.0889 ($C_5H_2N_3$) is consistent with the breakdown of a triazole ring or a nitrogen-rich aromatic moiety. Additionally, the ion at *m/z* 102.1247 (C_8H_5) suggests the loss of a small hydrocarbon fragment from the aromatic system. These fragmentation patterns collectively support the proposed degradation mechanism (Figure 5).

The less polar DP was noticed as **DP 5** at an RRT of 1.576 in the oxidative degradation chromatogram of futibatinib. The mass spectrum of DP 5 shows an increase in mass by approximately +16 Da, corresponding to standard futibatinib. This increase in mass value is due to the addition of one oxygen due to the oxidation of the $-NH_2$ group to the $-N=O$ group (nitroso group) by peroxide-induced degradation. The experimental mass spectrum has a peak for the molecular ion at *m/z* 433.4311 $[M+H]^+$, and this corresponds with the suggested molecular formula $C_{22}H_{20}N_6O_4$, which indicates the presence of an additional oxygen atom over that of the parent compound. The MS/MS fragmentation pattern also validates the structure of DP 5. A major fragment at *m/z* 258.2878 ($C_{14}H_{15}N_3O_2$) indicates cleavage at the oxidized amine region that points to a stable portion of the molecule intact after nitroso modification. Another prominent fragment at *m/z* 297.2603 ($C_{14}H_{10}N_5O_3$) validates the presence of a nitrogen-rich core from the incorporation of oxygen functionalities due to the nitroso group. The fragment at *m/z* 191.2179 ($C_{11}H_{12}NO_2$) indicates a cleaved moiety that contains both nitrogen and oxygen atoms, further confirming the oxidative modification. Additional ions at *m/z* 165.1441 ($C_6H_6N_5O$), 126.1446 ($C_7H_9O_2$), and 108.1133 ($C_5H_5N_3$) were noticed, represents smaller heterocyclic and aromatic fragments that confirm the preservation of other functional moieties from the parent structure. The MS/MS data of DPs characterized in this study were presented in Table 2, and the proposed mechanism of fragmentation was presented in supplementary files S7.

The structural elucidation of DPs was carried primarily using LC–MS/MS fragmentation data. The orthogonal techniques such as NMR were not employed to elucidate the structure of DPs due to limited sample availability and instrumental access. Hence these proposed structures were considered as putative assignments with moderate confidence and further study need to conduct to confirm the structure of DPs through comprehensive spectroscopic analyses.

Assessment of *in-silico* toxicity

In-silico prediction of toxicity was done to analyze the possible safety concerns of futibatinib DPs identified in this research. This involves the analysis of different endpoints of toxicity along with LD_{50} values and classification of tox-

Table 2. Identification and characterization of DPs of futibatinib formed under stress conditions using MS/MS analysis.

Name	Experi-mental *m/z* [M+H]$^+$	Theoretical mass *m/z* [M+H]$^+$	Proposed Molecular formula	Error (ppm)	*m/z* of major Fragments	Proposed Formula	Proposed structure
DP 1	319.7617	319.7615	$C_{14}H_{15}ClN_6O$	0.625	293.7430	$C_{13}H_{15}ClN_5O$	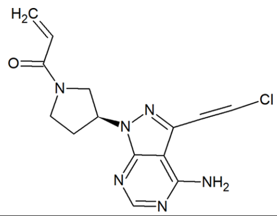
					239.6965	$C_{10}H_{13}ClN_5$	
					226.2291	$C_{11}H_9N_6$	
					202.2070	$C_9H_9N_6$	
					161.6244	$C_6H_{11}ClN_3$	
					112.1248	$C_4H_7N_4$	
DP 2	391.3954	391.3953	$C_{20}H_{20}N_6O_3$	0.255	283.2770	$C_{14}H_{12}N_5O_2$	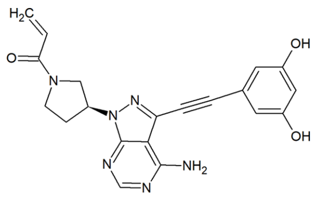
					231.2424	$C_{12}H_{12}N_3O_2$	
					163.1642	$C_9H_8O_2$	
					151.1610	$C_6H_8N_5$	
					112.1805	$C_6H_7O_2$	
					111.1361	$C_5H_8N_3$	
DP 3	365.4013	365.4011	$C_{19}H_{20}N_6O_2$	0.547	310.3221	$C_{16}H_{15}N_5O_2$	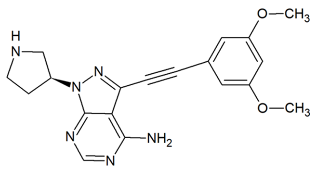
					229.2534	$C_{11}H_{12}N_6$	
					174.1750	$C_8H_7N_5$	
					134.1501	$C_7H_7N_3$	
					124.1350	$C_5H_7N_4$	
DP 4	296.2961	296.2960	$C_{15}H_{13}N_5O_2$	0.338	242.2450	$C_{13}H_{11}N_3O_2$	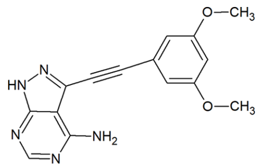
					162.1770	$C_{10}H_9O_2$	
					105.0885	$C_5H_2N_3$	
					102.1250	C_8H_5	
DP 5	433.4321	433.4320	$C_{22}H_{20}N_6O_4$	0.231	297.2605	$C_{14}H_{10}N_5O_3$	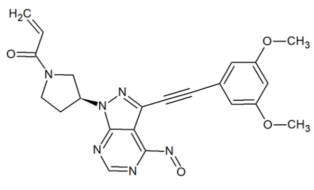
					258.2876	$C_{14}H_{15}N_3O_2$	
					191.2180	$C_{11}H_{12}NO_2$	
					165.1444	$C_6H_6N_5O$	
					126.1442	$C_7H_9O_2$	
					108.1131	$C_5H_5N_3$	

icity.[19] All the DPs were classified under toxicity class 4 which indicates moderate acute toxicity, with LD_{50} values of 1600 mg/kg for DP 1, DP 2, DP 3, and DP 5, while DP 4 shows slightly higher toxicity with an LD_{50} of 900 mg/kg. Among the endpoints of toxicity, neurotoxicity and carcinogenicity were predicted as active in all DPs, suggesting possible threats to the nervous system and possible cancer-causing activity. The respiratory toxicity was predicted in DP 1, DP 2, DP 3, and DP 5, while DP 4 exhibits inactive status, suggesting that it can be less likely to affect respiratory health. The hepatotoxicity was predicted as active only in DP 4, suggesting the possible liver damage risks specific to this DP. The nephrotoxicity observed only in DP 2 indicates a potential renal toxicity concern. The toxicity that represents genetic mutations, namely mutagenicity was predicted to be active in both DP 4 and DP 5, whereas the immunotoxicity was predicted for DP 2 and DP 3. Notably, all five predicted DPs to cross the blood-brain barrier indicate that these DPs have an enhanced risk of central nervous system-related side effects. All DPs were also predicted to be clinically toxic and non-nutritionally toxic, but none of them showed cardiotoxicity, cytotoxicity, or ecotoxicity. These results highlight the necessity of experimental confirmation and rigorous monitoring of these DPs in drug formulations for patient safety. The *in-silico* toxicity results of the present study are preliminary and require cautious interpretation until validated experimentally. Hence further study needs to conduct with a special focus to confirm the toxicity predictions through *in-vitro* and *in-vivo* assays.

Conclusions

In the present investigation, a stable, selective, and stability-indicating RP-HPLC technique was developed and validated successfully for the determination of futibatinib, its known impurities, and DPs. The technique exhibits satisfactory chromatographic performance with a Kinetex C18 column and an isocratic mobile phase system of acetonitrile and aqueous phosphate buffer (pH 4.1) in a ratio of 65:35 v/v. The maximum resolution of all analytes, including five DPs (DP 1 – DP 5), was obtained under a 12-minute runtime that reflects the appropriateness of the method to routine quality control and stability determination of futibatinib formulations. Forced degradation studies ascertain that futibatinib is specifically vulnerable to acidic and oxidative stress, resulting in structurally different degradation products. The kinetic investigation identified pseudo-first-order degradation characteristics with greater degradation under acidic conditions than under oxidative stress. The structural characterization by LC-MS/MS and HRMS reveals the primary degradation pathways as electrophilic Markovnikov-type addition, demethylation, hydrolysis, ring opening, and oxidation of the amine. The *in-silico* toxicity profiling of the purified DPs shows significant toxicological profiles. All the DPs were found to be neurotoxic and carcinogenic. DP 4 had the most serious toxicity profile with the lowest predicted LD_{50} (900 mg/kg). These findings highlight the urgent need for accurate control of degradation pathways during drug development and storage, and careful evaluation of the safety profiles of the degradative materials.

Acknowledgments

The authors are thankful to the Department of Chemistry, GITAM Institute of Science, GITAM (Deemed to be University), Visakhapatnam.

References

1. Prasad, S. S.; Kasimala, B. B.; Anna, V. R. *J. Chem.* **2021,** 14, 4, 2183-2190 http://doi.org/10.31788/RJC.2021.1446426
2. Kasimala, B. B.; Anna, V. R.; Mallu, U. R. *Pharm. Lett.* **2014,** 6, 4, 411–419.
3. Syed, Y. Y. *Drugs.,* **2022**, 82, 18, 1737–1743 https://doi.org/10.1007/s40265-022-01806.
4. Javle, M.; King, G.; Spencer, K.; Borad, M., J. *Oncol.* **2023**, 28, 11, 928-943 https://doi.org/10.1093/oncolo/oyad149.
5. Bairam, R.; Tatapudi, H. K.; Pothula, V. S.; Akaram, L.; Tummala, S. R.; Gorrepati, N.. *Lett. Appl. NanoBioSci.* **2024,** 14, 1, 1–12 https://doi.org/10.33263/LIANBS141.048.
6. Crolley, V.; Bridgewater, J., *Crit. Rev. Oncol. Hematol.* **2024,** 20, 1, 12–19 https://doi.org/10.17925/OHR.2024.20.1.4.
7. International Conference of Harmonisation. ICH. Q1A(R2), stability testing of new drug substances and products, 2003.
8. Jogeswararao, P.; Bhikshapathi, D. V. R. N. *Int. J. Pharm. Qual. Assur.*, **2023,** 14, 4.
9. Tang, L. W. T.; Chan, E. C. Y., *J. Pharm. Biomed. Anal.* **2022,** 214, 114731 https://doi.org/10.1016/j.jpba.2022.114731.
10. Li, H.; Ding, H.-Z.; Wang, Y.-L.; Zhang, F.; Song, Y.-H.; Qiu, X.-J., *J. Chem.* **2022,** 1, 1–7. https://doi.org/10.1155/2022/8316403.
11. Dadge, S. D.; Yadav, S.; Rathaur, S.; Gayen, J. R. *Biomed. Chromatogr.* **2024**, 38, 11, e6005. https://doi.org/10.1002/bmc.6005.
12. Tummala, S. R.; Amgoth, K. P. *Turk. J. Pharm. Sci.* **2022**, 19, 4, 455-461. https://doi.org/10.4274/tjps.galenos.2021.17702.
13. Bhupatiraju, R. V.; Kasimala, B. B.; Nagamalla, L.; Sayed, F. *Anal. Sci. Technol.* **2024**, 37, 2, 98-113 https://doi.org/10.5806/AST.2024.37.2.98.
14. ICH harmonised tripartite guideline stability testing of new drug substances and products Q1A(R2), 2003, 1-24.
15. Tummala, S. R.; Gorrepati, N.; Tatapudi, H. K. *Curr. Pharm. Anal.* **2024,** 20, 8, 944–952 https://doi.org/10.2174/0115734129332940240919113159.
16. Bhupatiraju, R. V.; Peddi, P.; Edla, S.; Rekha, K.; Kasimala, B. B. *Sep. Sci. Plus.* **2024**. https://doi.org/10.1002/sscp.202400106.
17. Bhupatiraju, R. V.; Peddi, P.; Tangeti, V, S.; Rao, B. S. *Anal. Sci. Technol.* **2024,** 37, 5, 280-294 https://doi.org/10.5806/AST.2024.37.5.280.
18. Amgoth, K. M.; Tummala, S. R. *J. Res. Pharm.* **2022**, 26**,** 6, 1685-1693 https://doi.org/10.29228/jrp.259.
19. Shaik, R. B.; Devi, D. R.; Basavaiah, K.; Rao. B. M. *Sep. Sci. Plus.* **2025**, 8, e70001. https://doi.org/10.1002/sscp.70001.